Local Heat Transfer Coefficient Measurements on Shaft Spray Cooled End Windings

Felix Hoffmann* , Jonas Bender† , Mattis Parche* , Thomas Wetzel† , Martin Doppelbauer*

* *Institute of Electrical Engineering (ETI), Karlsruhe Institute of Technology (KIT)*

† *Institute of Thermal Process Engineering (TVT), Karlsruhe Institute of Technology (KIT)*

Kaiserstr. 12, 76131 Karlsruhe, Germany

felix.hoffmann@kit.edu

***Abstract*—High power density electrical machines are mainly limited due to their cooling system. Oil spray cooled end windings are one possibility to significantly increase the power density. However, foundations for the estimation of the cooling capability are rather scarce in the design process. Different approaches to estimate the global heat transfer coefficients for spray cooled end windings exist in literature. However, local heat transfer coefficients, which are essential for the prediction of hot spots, can not be estimated. In this contribution, we present local heat transfer coefficient measurements for shaft spray cooled end windings. It is shown that the existence of a sump remarkably lowers the heat transfer coefficient, whereas it is almost constant over the remaining circumference. The rotational speed has a minor influence on the heat transfer. The latter is only increasing for very high speeds. A modeling approach for the Nusselt number is developed to apply it to different coolants. The achieved mean absolute percentage error between experimental and modeled Nusselt is $10.8\,\%$.**

***Index Terms*—spray cooling, direct cooling, heat transfer, heat transfer coefficients, electrical machines**

I. Introduction

Conventional cooling methods like water cooling jackets reach their limit in high power density machines [1]. A direct oil spray cooling of the end windings is one possibility to significantly increase the heat dissipation compared to an air cooling of the end windings [2]. In addition, a more homogeneous heat dissipation can be achieved [3], which leads to a more homogeneous temperature distribution, resulting in a reduced aging process of the insulation lacquer. Three different ways of direct oil spray cooling can be found in literature. The first two options use atomization or orifice-like nozzles to spray the oil either from the bearing shields in axial direction to the end windings [4]–[6] or from the housing in radial direction to the end windings [2]. In case of an atomization of the cooling fluid, the cooling capability can be increased under certain process conditions [7]. The last option is to use the centrifugal force to spray the fluid from the shaft to the end windings [8]. All contributions exclusively focus on the global heat transfer coefficients (HTC) by dertermining the total transfer rate between end windings and coolant. However, the work of [2] indicates that the locally varying fluid distribution leads to an inhomogeneous HTC distribution. These inhomogeneous HTC distributions can not be measured with the measurement principles presented in literature. There also exist different modeling approaches for the Nusselt number of liquid impingement jets in literature [9]–[13] and therefore to calculate the HTC depending on the fluid properties and operating conditions. [13] averages the HTC of the jet over a curved surface, which is similar to an end winding geometry. However, none of the approaches consider a rotational movement of the nozzle orifice as it is present in the case of shaft spray cooling. All measurements are performed in static conditions and the same location is sprayed continuously, whereas in an electrical machine, the surface is only sprayed for a certain amount of time throughout one rotation of the shaft. In this paper, we will present an approach to measure the local HTC for a shaft spray cooling considering a rotating shaft, which is particularly important to estimate hot spots in an electrical machine. Measurements at different azimuthal positions, varying rotational speeds, different fluid temperatures and different volumetric inlet flows are presented. In addition, a modeling approach of the Nusselt number for shaft spray cooled end windings is presented.

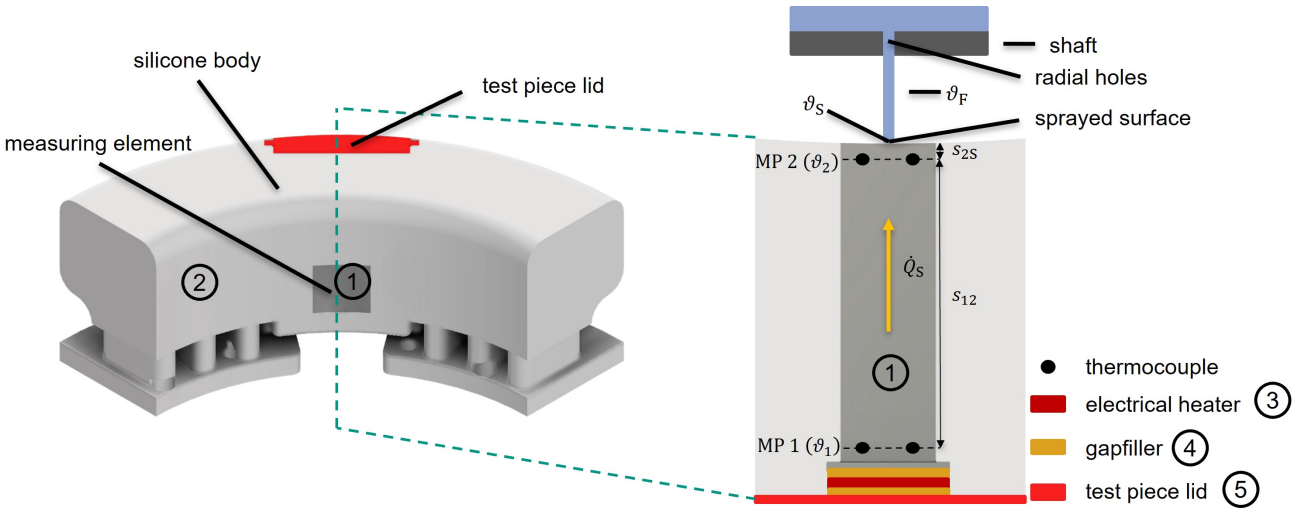

Fig. 1. Whole test piece (left) and sectional view of measuring principle (right), modified from [14].

II. Measurement Concept

A. Measurement Principle

Fig. 1 shows the measurement principle. To measure local HTCs, small measuring elements (MEL) (1) made of an aluminum alloy are placed in a silicone body (2). A predefined heat flux is generated by an electrical heater (3) and transferred into the measuring element. Gap fillers (4) and a thermoplastic lid (5) mounted at the bottom of the heater are used to reduce thermal contact resistances. The temperature inside the measuring element is measured in two planes MP1 and MP2 using thermocouples of type K. By knowing the exact distance between those two planes s_{12} and knowing the thermal conductivity λ_{12} of the measuring element, the exact heat flux $\dot{Q}_S$ can be determined. Knowing the heat flux $\dot{Q}_S$, temperature ϑ_2 and the distance from the upper measuring plane MP2 to the sprayed surface s_{2S}, the surface temperature ϑ_S can be extrapolated. The fluid temperature ϑ_F is measured with a PT1000 temperature sensor. With all these parameters the HTC can be calculated similar to [14]:

$$HTC = \frac{\dot{Q}_S}{A_S \cdot (\vartheta_S - \vartheta_F)} \tag{1}$$

$$= \frac{\lambda_{12}}{s_{12}} \cdot \frac{(\vartheta_1 - \vartheta_2)}{\left(\vartheta_2 - \frac{s_{2S}}{s_{12}} \cdot (\vartheta_1 - \vartheta_2) - \vartheta_F\right)}, \tag{2}$$

where ϑ_1 and ϑ_2 denote the measured temperature in plane 1 and plane 2 and A_S describes the area of the sprayed surface of the measuring element. By changing the sprayed surface of the measuring element, the spatial discretization of the measurement of the local HTC is changed. In the presented setup the dimension of the projected area of the concave measuring element is $12.7\,\mathrm{mm}$ x $12.7\,\mathrm{mm}$. The measurement uncertainty was determined according to GUM-B [15].

B. Model Fluid Concept

In traction applications several different transmission oils are used. Depending on the temperature and on the used oil, the fluid properties vary and hence the HTC will change. In order to cover a broad range of transmission oils, a model fluid concept was developed [14]. A binary mixture of glycerol and water was used in this case, where the temperature and composition is adjusted in a way to cover transmission oils in their relevant operating range ($60\,^\circ\mathrm{C}$ - $90\,^\circ\mathrm{C}$). The mapping is based on two dimensionless numbers: The Prandtl number Pr, which describes the thermal transport process during spray cooling. It is calculated by

$$Pr = \frac{\eta_F \cdot c_p}{\lambda_F}, \tag{3}$$

where η_F denotes the dynamic viscosity of the fluid, c_p the specific heat capacity and λ_F the thermal conductivity of the fluid. The Ohnesorge number, which describes the atomization during the spray process, is given by

$$Oh = \frac{\eta_F}{d_0 \cdot \rho_F \cdot \sigma_F}, \tag{4}$$

where d_0 describes the characteristic length, which is the diameter of the radial shaft holes, ρ_F describes the density

of the fluid and σ_F describes the surface tension of the fluid. Both dimensionless numbers are independent from operating conditions and therefore primarily represent the influence of the fluid properties.

III. Machine Under Test

In order to measure local HTCs, the measurement principle, explained in section II-A, is used in an electrical machine. The measuring element has a curvature according to the inner diameter of the end windings and the surrounding silicone structure corresponds to the shape of an end winding (compare Fig. 1). However, simplifications are required to embed the measuring principle. The air spaces between two coils are chosen according to a real winding structure. Fig. 2 shows a CAD-view of the used generic electrical machine including the test piece and Fig. 3 the generic machine and its assembly at the test bench including the fluid loop. The local HTCs are measured simultaneously at four locations, separated by $90°$ to each other. The whole structure is mounted at the end of the axial length of the stator and can be freely rotated to measure the HTCs along the circumference. The machine is designed with a rotor diameter of $108\,\mathrm{mm}$, an inner stator diameter of $110\,\mathrm{mm}$ and an outer stator diameter of $180\,\mathrm{mm}$. Therefore, the silicone structure was designed with an inner diameter of $115\,\mathrm{mm}$ and an outer diameter of $175\,\mathrm{mm}$. The air spaces of the silicone structure are built according to a machine with three pole pairs and 36 slots. Four radial holes separated by $90°$ in the shaft with a diameter of $1\,\mathrm{mm}$ are used for the spray cooling. The design of the radial holes is done according to [16]. In axial direction they are placed in the center of the end winding structure, which has a total height of $45\,\mathrm{mm}$. To measure the effect of the rotational speed, the generic machine is driven by an external drive, which can reach speeds up to $10.000\,\mathrm{min^{-1}}$. The fluid is fed to only one end region of the machine to avoid the effect of an unequal distribution of the fluid to both end regions. The fluid is collected in a tank right below the electrical machine and is fed back to the thermostat by a gear pump. The water glycerol mixture with mass percentage of water of approximately $11\,\%$ is used at temperatures between $\vartheta_F = 54\,°\mathrm{C}$ and $\vartheta_F = 68\,°\mathrm{C}$. This range represents the same Prandtl numbers as transmission oils in the range of $60\,°\mathrm{C}$ up to $90\,°\mathrm{C}$. HTCs for a maximum volumetric inlet flow per hole of $0.7\,\mathrm{l/min}$ are measured, which equals a system volumetric inlet flow of $5.6\,\mathrm{l/min}$ considering four radial holes on the front and rear side of the machine.

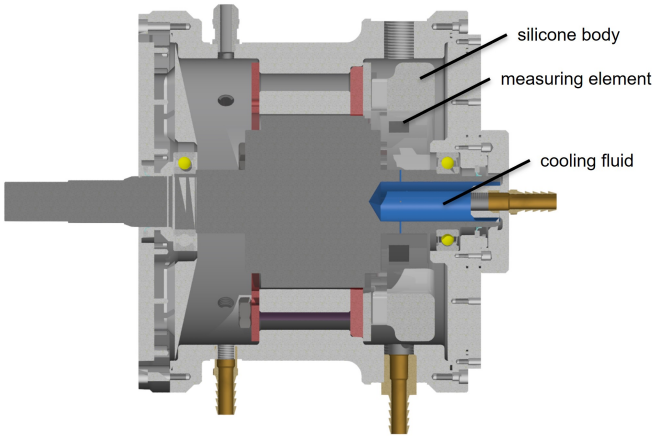

Fig. 2. Sectional view of the CAD-model of the used generic machine

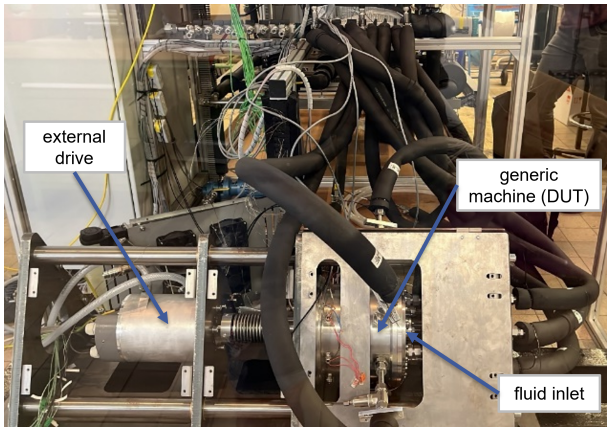

Fig. 3. Generic machine assembled at the test bench.

IV. Measurement Results

All measurements were performed with a water glycerol mixture with a mass percentage of water of approximately $11\,\%$. In a first step, the dependency of the rotational speed on the HTC is observed. Fig. 4 shows the measurement results for a volumetric inlet flow per hole of $\dot{V} = 0.6\,\mathrm{l/min}$, a varying rotational speed from $-10\,000\,\mathrm{min^{-1}}$ up to $10\,000\,\mathrm{min^{-1}}$ and a fluid temperature of $\vartheta_F = 54\,°\mathrm{C}$ and $\vartheta_F = 68\,°\mathrm{C}$. The measurement angles are declared in clockwise direction. The HTCs exhibit no dependence on the direction of rotation. The measuring element on the bottom at $180°$ shows significant smaller HTCs compared to the other ones. This is due to the fact that a sump is present in this case, covering the

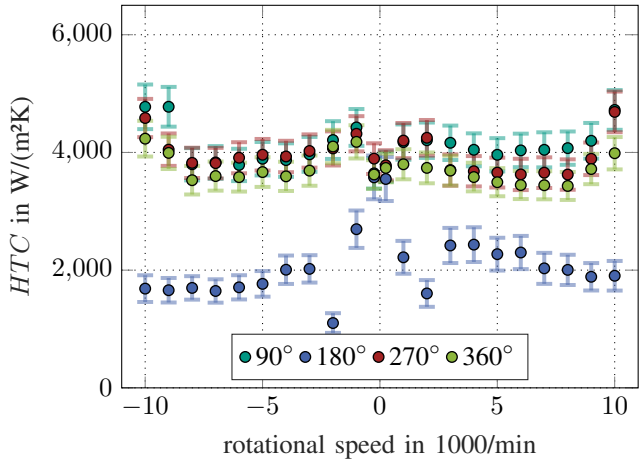

(a) fluid temperature $\vartheta_F = 54\,°C$

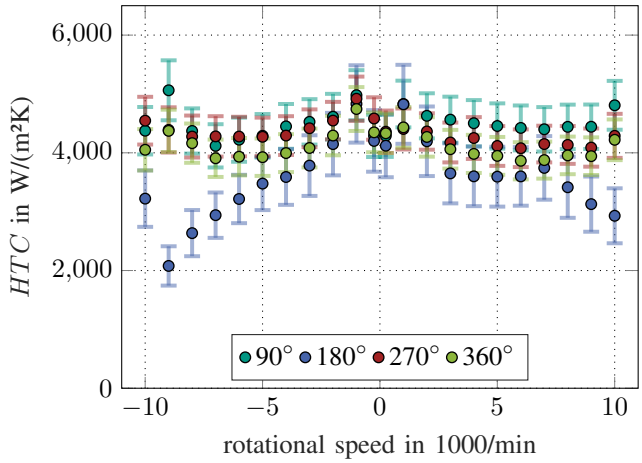

(b) fluid temperature $\vartheta_F = 68\,°C$

Fig. 4. HTC for a volumetric inlet flow per hole of $\dot{V} = 0.6\,l/min$ at measuring angles of $\phi = [90°\ 180°\ 270°\ 360°]$ and a varying rotational speed from $-10\,000\,min^{-1}$ up to $10\,000\,min^{-1}$.

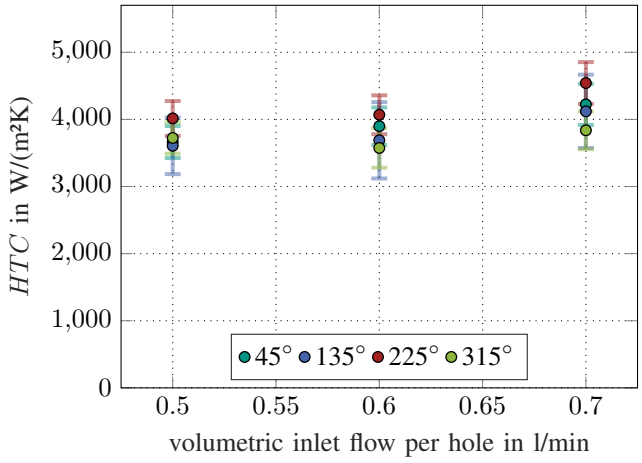

(a) measuring angles of $\phi = [45°\ 135°\ 225°\ 315°]$

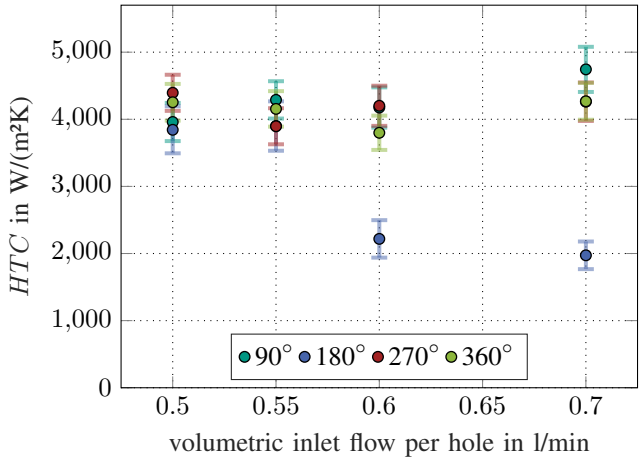

(b) measuring angles of $\phi = [90°\ 180°\ 270°\ 360°]$

Fig. 5. HTC for a fluid temperature of $\vartheta_F = 54\,°C$ at a speed of $n = 1000\,min^{-1}$ for different measurement angles and a varying volumetric inlet flow per hole from $\dot{V} = 0.5\,l/min$ up to $\dot{V} = 0.7\,l/min$.

measuring element and leading to a lower heat transfer. For a higher fluid temperature the HTC is increasing due to a higher Reynolds number and the sump is lower due to a lower dynamic viscosity of the fluid, leading to a better outflow. It can also be seen that the HTC increases from standstill up to about $1000\,min^{-1}$, followed by a decline up to a rotational speed of $8000\,min^{-1}$ and a renewed increase for higher speeds. A plausible cause for the observed trends is the increasing kinematic energy of the droplets with increasing speed. The decrease between $1000\,min^{-1}$ and $8000\,min^{-1}$ results from a higher amount of gas in the fluid, whereas the rise of kinematic energy becomes predominant again above $8000\,min^{-1}$. As a next step, the influence of the volumetric inlet flow is observed. Fig. 5 shows the result at a rotational speed of $1000\,min^{-1}$, a changing volumetric inlet flow per hole from $\dot{V} = 0.5\,l/min$ up to $\dot{V} = 0.7\,l/min$ and different measuring angles. It can be seen directly that the HTCs increase with an increasing volumetric inlet flow due to an enlarged Reynolds number except for the measuring element at 180°, which corresponds to the one in the sump. The height of the sump increases with an increasing volumetric inlet flow leading to a lower HTC. Therefore, it is not always beneficial to increase the volumetric inlet flow. As a last point, the HTC is observed along the circumference. Fig. 6 shows the results for a volumetric inlet flow per hole of $\dot{V} = 0.5\,l/min$ and $\dot{V} = 0.6\,l/min$, a fluid temperature of $\vartheta_F = 54\,°C$ and a rotational speed of $4000\,min^{-1}$. All measured heat transfer coeffiecients

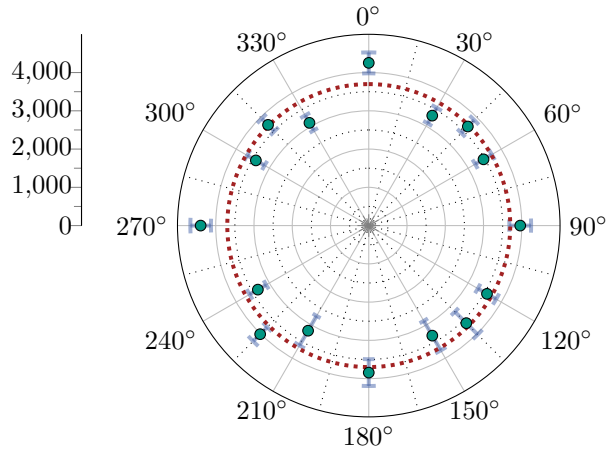

(a) volumetric inlet flow per hole $\dot{V} = 0.5\,\mathrm{l/min}$

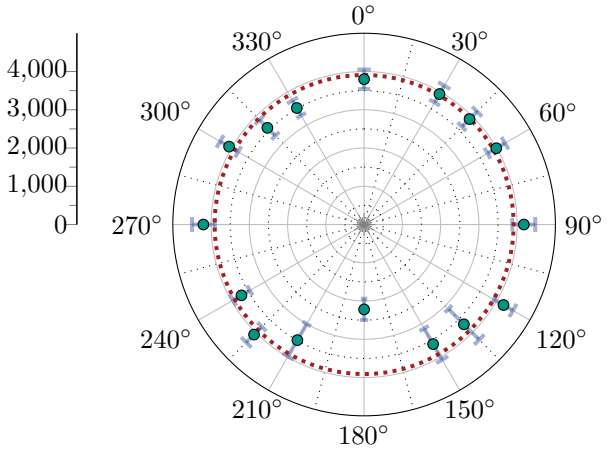

(b) volumetric inlet flow per hole $\dot{V} = 0.6\,\mathrm{l/min}$

Fig. 6. HTC distributed over the circumference for a fluid temperature of $\vartheta_\mathrm{F} = 54\,^\circ\mathrm{C}$ at a speed of $n = 4000\,\mathrm{min}^{-1}$ and average HTC (red).

are within the measurement uncertainty not changing over the circumference for a volumetric inlet flow per hole of $\dot{V} = 0.5\mathrm{l/min}$. For a volumetric inlet flow per hole of $\dot{V} = 0.6\mathrm{l/min}$ the influence of the sump is visible again at a measurement angle of 180° resulting in a lower HTC.

V. Modeling

As a last part, the measurement results are modeled in a way that they are applicable to other fluids, including commercial transmission oils. There are several approaches in literature, which model the Nusselt number of oil impingement jets [9]–[13]. However, the measuring element in our case is not sprayed continuously as the shaft and thus also the jet rotates. There is no known modeling approach for a rotating spray source. To consider the relative time the measuring element is sprayed, a spray ratio is defined in the modeling approach, which is given by

$$ratio_\mathrm{spray} = \sin^{-1}\left(\frac{b_\mathrm{MEL}}{d_\mathrm{in,Stator}}\right) \cdot \frac{num_\mathrm{holes}}{\pi}, \tag{5}$$

where b_MEL defines the width of the projected area of the concave measuring element, $d_\mathrm{in,Stator}$ the inner diameter of stator end winding and num_holes the number of radial holes in the shaft in one end region. In the present machine the $ratio_\mathrm{spray}$ is given by 0.14. The overall modeling approach is based on a Re, Pr power law function typical for impingement jet correlations as well as spray cooling correlations [14]. This leads to the following general structure of the Nusselt correlation

$$Nu = ratio_\mathrm{spray} \cdot a \cdot Re^b \cdot Pr^{\frac{1}{3}}, \tag{6}$$

where a and b define the coefficients of the correlation, which need to be fitted to the measurement data. Pr denotes the Prandtl number given by (3) and Re denotes the Reynolds number given by

$$Re = \frac{v_\mathrm{F} \cdot d_0 \cdot \rho_\mathrm{F}}{\nu_\mathrm{F}}. \tag{7}$$

The fluid velocity v_F is for a rotating shaft also dependent on the rotational speed and can be expressed by

$$v_\mathrm{F} = \sqrt{\left(\frac{\dot{V}}{\frac{\pi \cdot d_0^2}{4}}\right)^2 + \left(\omega_\mathrm{rot} \cdot r_\mathrm{shaft}\right)^2}, \tag{8}$$

where $\dot{V}$ expresses the volumetric inlet flow per hole, ω_rot the angular velocity of the shaft and r_shaft the outer radius of the shaft. Fig. 7 shows the Nusselt number times the Prandtl number to the power of -1/3 as a function of the Reynolds number for all measured data points. The Prandtl number to the power of -1/3 is used to reduce the dependencies of the measured data to the influence of the Reynolds number. In addition, a model fit is shown, which was achieved by a least squares algorithm omitting the measured heat transfer coefficients influenced by a sump. Including the measurements where a sump was present, would significantly change the obtained correlation. The different measuring elements are indicated by different colors. The resulting Nusselt correlation leads to

$$Nu = spray_\mathrm{ratio} \cdot 2.29 \cdot Re^{0.28} \cdot Pr^{1/3}. \tag{9}$$

The modeling approach has a mean absolute percentage error of $10.8\,\%$ between experimental and modeled Nusselt number.

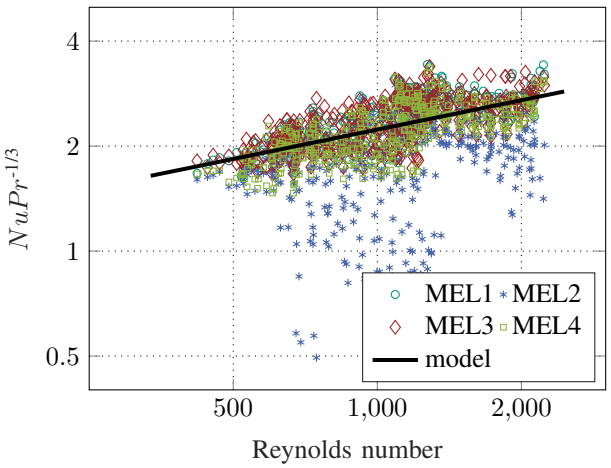

Fig. 7. $NuPr^{-1/3}$ over Reynolds number in logarithmic scale for all observed measurement data of the measuring elements and the devoloped modeling approach (black). The different measuring elements are indicated by different colors.

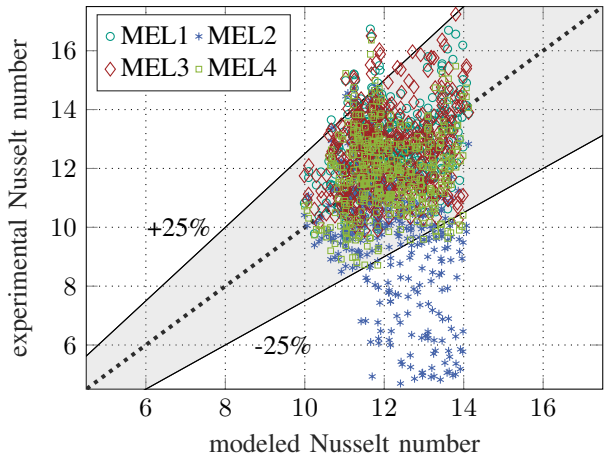

Fig. 8. Experimental Nusselt number over modeled Nusselt number according to (9) for all measurement data and a confidence interval of 25 %. The different measuring elements are indicated by different colors.

To get another representation of the modeling approach, Fig. 8 shows a parity plot of the experimental Nusselt number over the modeled Nusselt number according to (9) for all measurement data. In addition, a confidence interval of 25 % is shown. Only 6.9 % of the measurement points are outside the confidence interval of 25 % in addition to measurements, where a sump is present. These measurements show a lower experimental Nusselt number compared to the modeled Nusselt number, which was also observed in the previous measurement results like in Fig. 4 (a). A confidence interval of 25 % is a well accepted uncertainty for HTC measurements and can therefore be applied to the end windings of electrical machines. However, it should be noted that a variation in spray distance, an axial displacement between the measuring element and the radial shaft holes as well as a variation of the inner stator diameter was not performed in the shown measurements. Therefore it is recommended to restrict the applicability of correlation to the investigated parameters even though it is shown in [12] that the spray distance has a minor influence on the HTC. In the design process, care must be taken when applying the correlation to ensure that no sump is present.

VI. Conclusion and Future Work

In this paper we have presented a local HTC measurement setup for shaft spray cooled end windings in electrical machines. It was shown that a sump is build up at the bottom of the observed machine for higher volumetric inlet flows, which lowers the local HTC significantly, whereas the HTCs are constant over the remaining circumference. The rotational speed has a minor influence on the HTC. A dimensionless heat transfer model using the Nusselt number is presented, which allows for the transfer of the measured data to various coolants. The model has a mean absolute percentage error of 10.8 % and 93 % of all measurement data lie in a confidence interval of 25 %. With the developed model, it is possible to calculate the heat transfer coefficients depending on the fluid properties and directly feed it to a thermal model, which can be used in the design process of electrical machines.
The variation of the spray distance, the stator inner diameter and an axial displacement between measuring element and radial shaft holes was not observed in the measurement setup and is part of our future work to validate the developed modeling approach.

Acknowledgment

The authors would like to thank the German Federation of Industrial Research Associations (AiF) for funding the project “SprayCEM” (IGF-Nr. 20913 N) as part of the IGF program of the BMWK as well as the supporting project committee within the FVA.

References

[1] A. Boglietti, A. Cavagnino, and D. Staton, “Determination of critical parameters in electrical machine thermal models,” *IEEE Transactions on Industry Applications*, vol. 44, no. 4, pp. 1150–1159, 2008.

[2] T. Davin, J. Pellé, S. Harmand, and R. Yu, "Experimental study of oil cooling systems for electric motors," *Applied Thermal Engineering*, vol. 75, pp. 1–13, 2015.

[3] J. Kim, "Spray cooling heat transfer: The state of the art," *International Journal of Heat and Fluid Flow*, vol. 28, pp. 753–767, 2007.

[4] F. Zhang, D. Gerada, Z. Xu, C. Liu, H. Zhang, T. Zou, Y. C. Chong, and C. Gerada, "A thermal modelling approach and experimental validation for an oil spray-cooled hairpin winding machine," *IEEE Transactions on Transportation Electrification*, p. 1, 2021.

[5] C. Liu, Z. Xu, D. Gerada, J. Li, C. Gerada, Y. C. Chong, M. Popescu, J. Goss, D. Staton, and H. Zhang, "Experimental investigation on oil spray cooling with hairpin windings," *IEEE Transactions on Industrial Electronics*, vol. 67, no. 9, pp. 7343–7353, 2020.

[6] C. Liu, D. Gerada, Z. Xu, Y. C. Chong, M. Michon, J. Goss, J. Li, C. Gerada, and H. Zhang, "Estimation of oil spray cooling heat transfer coefficients on hairpin windings with reduced-parameter models," *IEEE Transactions on Transportation Electrification*, p. 1, 2020.

[7] G. Liang and I. Mudawar, "Review of spray cooling – part 1: Single-phase and nucleate boiling regimes, and critical heat flux," *International Journal of Heat and Mass Transfer*, vol. 115, pp. 1174–1205, 2017.

[8] B. Assaad, K. Mikati, T. V. Tran, and E. Negre, "Experimental study of oil cooled induction motor for hybrid and electric vehicles," in *2018 XIII International Conference on Electrical Machines (ICEM)*, 2018, pp. 1195–1200.

[9] M. Molana and S. Banooni, "Investigation of heat transfer processes involved liquid impingement jets: a review," *Brazilian Journal of Chemical Engineering*, vol. 30, no. 3, pp. 413–435, 2013.

[10] C. Renon, M. Fénot, M. Girault, S. Guilain, and B. Assaad, "An experimental study of local heat transfer using high prandtl number liquid jets," *International Journal of Heat and Mass Transfer*, vol. 180, p. 121727, 2021.

[11] X. Liu, J. H. Lienhard, and J. S. Lombara, "Convective heat transfer by impingement of circular liquid jets," *Journal of Heat Transfer*, no. 113, pp. 571–593, 1991.

[12] J. Stevens and B. W. Webb, "Local heat transfer coefficients under an axisymmetric single-phase liquid jet," *Journal of Heat Transfer*, no. 113, pp. 71–78, 1991.

[13] J. Easter, C. Jarrett, C. Pespisa, Y. C. Liu, A. C. Alkidas, L. Guessous, and B. P. Sangeorzan, "An area-average correlation for oil-jet cooling of automotive pistons," *Journal of Heat Transfer*, no. 136, 2014.

[14] K. Dubil, J. Bender, F. Hoffmann, B. Dietrich, M. Doppelbauer, and T. Wetzel, "Single-phase convective heat transfer on spray cooled plain surfaces with high prandtl number liquids," *International Journal of Heat and Mass Transfer, accepted.*

[15] BIPM, IEC, IFCC, ILAC, ISO, IUPAC, IUPAP, and OIML, "Evaluation of measurement data — Guide to the expression of uncertainty in measurement," Joint Committee for Guides in Metrology, JCGM 100:2008. [Online]. Available: https://www.bipm.org/documents/20126/2071204/JCGM_100_2008_E.pdf/cb0ef43f-baa5-11cf-3f85-4dcd86f77bd6

[16] F. Hoffmann, K. Dubil, J. Bender, T. Wetzel, and M. Doppelbauer, "Operational design analysis of a shaft oil spray cooling in electrical machines," in *Energy Efficiency in Motor Driven Systems (EEMODS)*, 2022.

BIOGRAPHIES

Felix Hoffmann was born in Landau in der Pfalz, Germany. He received his B.Sc. and M.Sc. degrees in electrical engineering from the Swiss Federal Institute of Technology Zurich (ETH Zurich) in 2016 and 2018, respectively. He is currently working towards his Ph.D. degree at the Karlsruhe Institute of Technology (KIT) in the laboratory of hybrid electric vehicles (HEV). His research interests include the thermal analysis and thermal modeling of electrical machines.

Jonas Bender was born in Speyer, Germany. He received his B.Sc. and M.Sc. degrees in chemical engineering from the Karlsruher Institute of Technology (KIT) in 2017 and 2020, respectively. He is currently working towards his Ph.D. degree at the Karlsruhe Institute of Technology (KIT) at the Institute of Thermal Process Engineering (TVT). His research focuses on the experimental investigation of the heat transfer of spray-cooled electrical machines and the development of heat transfer models for these.

Mattis Parche was born in Stuttgart, Germany. He received his B.Sc. and M.Sc. degrees in Mechatronics and Information Technology from the Karlsruhe Institut of Technology (KIT) in 2019 and 2022, respectively. He is currently working towards his Ph.D. degree at the Karlsruhe Institute of Technology (KIT) at the Institute of Electrical Engineering (ETI). His research interests include the analysis and experimental investigation of electric machines.

Thomas Wetzel holds a full professorship for Heat and Mass Transfer at the Faculty of Chemical and Process Engineering of the Karlsruhe Institute of Technology (KIT). Before joining KIT, Prof. Wetzel held several R&D management positions in chemical and automotive industry companies. His research fields are single- and multi-phase heat transfer, thermal behaviour of Li-ion batteries and liquid metal thermal hydraulics for high temperature process technology and heat storage.

Martin Doppelbauer is full professor since 2011 at the Institute of Electrical Engineering (ETI) at the Karlsruhe Institute of Technology (KIT) in Karlsruhe, Germany. He holds a chair for Hybrid Electric Vehicles. Prior to that, he worked in industry for 15 years, most recently as head of electrical machine development at SEW Eurodrive GmbH in Bruchsal. Martin Doppelbauer is also active in national and international standardization. He is the chairman of IEC Technical Committee 2 Rotating Electrical Machines.